

Classical eigenvalue mode-spectrum analysis of multiple-ridged rectangular and circular waveguides for the design of narrowband waveguide components

Seng Yong Yu and Jens Bornemann^{*,†}

Department of Electrical and Computer Engineering, University of Victoria, Victoria, BC, Canada V8W 3P6

SUMMARY

A classical eigenvalue mode-spectrum analysis of waveguides with multi-ridged cross sections is presented and applied to the design of narrowband waveguide components in rectangular and circular waveguide technology. Modifications of the modes of the empty waveguide enclosures are used as expansion functions and lead to a classical, real and symmetric eigenvalue problem. A simple yet efficient constraint function is introduced to satisfy boundary conditions for TM modes. The number and locations of ridges positioned in a regular rectangular or circular waveguide enclosure is arbitrary. Measurements and comparisons with results from existing full-wave modeling tools and commercially available field solvers verify the correctness and flexibility of the approach. Copyright © 2009 John Wiley & Sons, Ltd.

Received 9 May 2008; Revised 8 September 2008; Accepted 27 January 2009

KEY WORDS: waveguide modes; irregular waveguides; classical eigenvalues; mode-matching techniques; computer-aided design

1. INTRODUCTION

Waveguide components in advanced satellite and communications systems as well as base-station equipment have utilized waveguides with nonstandard cross sections for a long time. Such cross sections typically include a variety of ridges in either rectangular enclosure, e.g. multiple-ridged waveguides [1–6], T-septum waveguides [6–9], L-shaped waveguides [10], trough waveguides [11], or in circular housings, e.g. multiple-ridged circular waveguides [1,5,12–15], and corrugated circular waveguides [16,17]. Moreover, a number of more arbitrarily shaped cross sections are frequently employed [18–21]. In order to incorporate such irregular

*Correspondence to: Jens Bornemann, Department of Electrical and Computer Engineering, University of Victoria, Victoria, BC, Canada V8W 3P6.

†E-mail: j.bornemann@ieec.org

waveguides into computer-aided design procedures for narrowband waveguide components, their mode sequences and related expansion coefficients must be known.

A popular approach to determine the modal distribution of irregular waveguides is to subdivide the cross section into subregions, e.g. [3–13,15], which leads to a singular-value problem requiring the system determinant or, alternatively, the smallest singular value to vanish [9]. However, this method has several disadvantages. Firstly, it requires a search algorithm to determine the mode spectrum, which is computationally expensive and lacks accuracy, especially if cut-off frequencies of modes are located very close together or are even identical within the smallest variation acceptable in the search. Secondly, if the cross-sectional dimensions are varied within an optimization run, the boundary conditions with respect to the subdivisions might change, thus requiring that the altered configuration be solved and coded separately. Thirdly, using different subdivision schemes, e.g. horizontal versus vertical, leads to slightly different results for an entire waveguide component containing such cross sections. This is demonstrated in [11]. It is therefore advisable to develop a method that refrains from dividing the entire cross section into subregions.

This is accomplished by setting up a classical eigenvalue formulation, e.g. [19,22–24], and selecting appropriate basis functions. The mode-matching-finite-element method, e.g. [25], is especially useful in this respect. One issue to consider, though, is whether or not the resulting eigenvalue equation requires complex arithmetic to be applied to asymmetric matrices. In this respect, the approach presented in [26–29] is advantageous since the resulting matrices are real and symmetric, and, in addition, the approach is easily combined with the three-dimensional mode-matching technique (MMT). However, the basis functions used in [26–29] are polynomials involving the computation of Gamma functions, which limits efficient code implementation. Therefore, only simple discontinuities have been presented so far [29] as they require only a limited number of eigenmodes to be considered in the irregular cross sections. For narrowband and highly frequency-dependent waveguide components, however, it is mandatory to compute reliably the cut-off frequencies and expansion coefficients of hundreds of modes in such cross sections.

Therefore, this paper focuses on a combination of the approaches used in [23] and [26–29]. We use the eigenmodes of the empty waveguide enclosures as basis functions, as proposed in [23], but refrain from limiting the numbers and locations of ridges by introducing edge conditions. And we apply the formulation of [26–29] in order to obtain a numerically friendly classical, real and symmetric eigenvalue equation. The only challenge is a constraint function to enforce the boundary condition for TM modes. However, as we demonstrate in the next section, this can be achieved straightforwardly and in a flexible yet easily implementable manner.

Moreover, the new eigenvalue mode-spectrum analysis has the following advantages: First, the number of ridges and their locations within a waveguide housing is arbitrary, and a division into subregions is not required. Second, all inner product calculations can be performed over the surface areas of the ridges so that integration over the actual, more complicated cross section of the irregular, multiple-ridged waveguide becomes unnecessary. Third, the power normalizations of the multi-ridged waveguide modes follow directly from the eigenvalue solutions and need not be recomputed. Fourth, two submatrices of the coupling matrix to the empty waveguide enclosure follow straightforwardly from the eigenvalue solutions. Only TM-to-TE-mode coupling must be recomputed.

This paper focuses on a more detailed description of the method compared with a recent conference contribution [30]. Moreover, we present convergence behavior, a number of new and

numerically more challenging examples and, for the first time, the related algorithm in the circular–cylindrical coordinate system including three examples.

2. THEORY

Figure 1 shows general cross sections of ridges in rectangular (Figure 1(a)) and circular (Figure 1(b)) waveguide housings. We restrict our investigations to structures involving pure TE and TM modes so that individual ridges must either share a common wall with the housing, or they are connected to each other with at least one of them connected to the housing.

Following the general approach presented in [26–29], we obtain the mode spectrum from

$$\nabla_T^2 \begin{Bmatrix} H_z \\ E_z \end{Bmatrix} + k_c^2 \begin{Bmatrix} H_z \\ E_z \end{Bmatrix} = 0 \tag{1}$$

where ∇_T is the transverse Laplacian operator, k_c are the eigenvalues to be determined, and H_z , E_z are the longitudinal field components of TE and TM modes, respectively. As we will demonstrate in the following subsections, the z components are expanded in basis functions, which either coincide with the eigenmodes of the waveguide enclosure (TE modes) or are modifications thereof (TM modes).

$$\begin{Bmatrix} H_z \\ E_z \end{Bmatrix} = \sum_{p=1}^P c_p \begin{Bmatrix} h_{zp} \\ e_{zp} \end{Bmatrix} \tag{2}$$

After testing (2) with the respective TE- or TM-mode spectra of the waveguide housing and truncating the series, a generalized eigenvalue equation is obtained.

$$[K]\underline{c} = \underline{k}_c^2 [M]\underline{c} \tag{3}$$

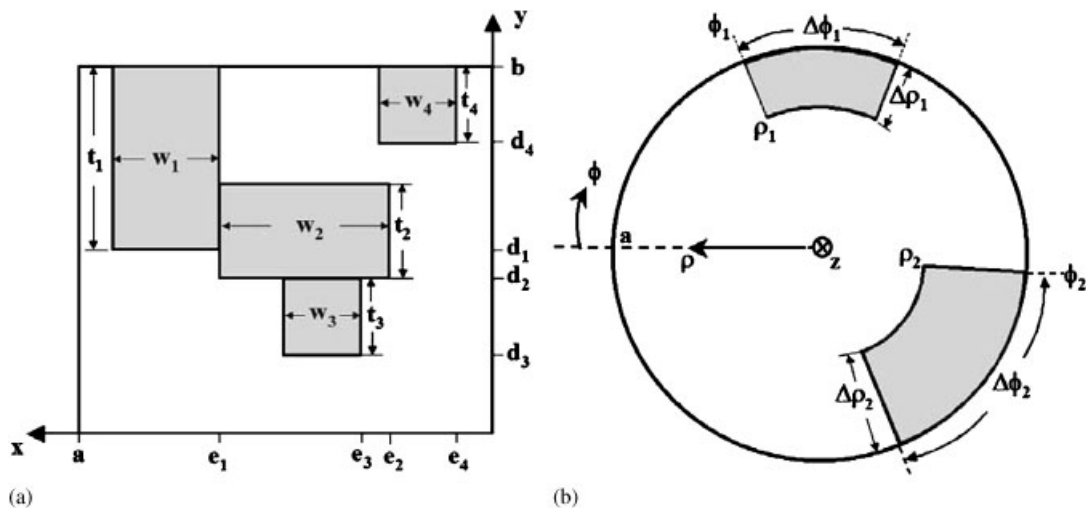


Figure 1. Cross sections of multiple ridges in rectangular waveguides: (a) four ridges in rectangular waveguide and (b) two ridges in circular waveguide.

Diagonal matrix \underline{k}_c holds P eigenvalues, which specify the first P cut-off frequencies f_{cp} . Matrix \underline{c} holds the corresponding eigenvectors. The matrix elements of K and M in (3) represent the inner products of the modes of the housing (T_p) with the expansions in (2).

$$K_{pq} = \int_S \nabla_T \left\{ \begin{matrix} T_{hp} \\ T_{ep} \end{matrix} \right\} \nabla_T \left\{ \begin{matrix} h_{zq} \\ e_{zq} \end{matrix} \right\} ds \quad (4a)$$

$$M_{pq} = \int_S \left\{ \begin{matrix} T_{hp} \\ T_{ep} \end{matrix} \right\} \left\{ \begin{matrix} h_{zq} \\ e_{zq} \end{matrix} \right\} ds \quad (4b)$$

Here, S represents the cross section of the irregular (ridged) waveguide. However, in order to maintain flexibility of the positions of all ridges, all surface integrals are computed as the difference between those over the empty housing and those over the N ridges within that housing.

$$\int_S f(s) ds = \int_{\text{housing}} f(s) ds - \sum_{i=1}^N \int_{\text{ridge}(i)} f(s) ds \quad (5)$$

Once the eigenvalues and eigenvectors are obtained from (3), each mode i of the multiple-ridged waveguide can be power normalized as required for a MMT computation in axial (z) direction.

$$P_i = k_{ci}^2 \sum_{p=1}^P M_{ip} c_{ip}^2 \quad (6)$$

As MMT routines are based on mode coupling between the modes of the empty waveguide and those of the ridged waveguide, a frequency-independent coupling matrix of the form

$$J = \begin{bmatrix} J_{hh} & 0 \\ J_{eh} & J_{ee} \end{bmatrix} \quad (7)$$

must be set up. It is one of the advantages of using empty waveguide modes as expansion functions that submatrices J_{hh} and J_{ee} are directly obtained from (4a).

$$(J_{hh})_{q,i} = A_q \sum_{p=1}^{P_h} (K_h)_{ip} (c_h)_{ip} \quad (8a)$$

$$(J_{ee})_{q,j} = D_q \sum_{p=1}^{P_e} (K_e)_{jp} (c_e)_{jp} \quad (8b)$$

Note that in (8), we have acknowledged the fact that the number of expansion terms P used in (2) are normally different for TE (P_h) and TM (P_e) modes with eigenvector matrices c_h and c_e , respectively. A_q and D_q are the well-known power normalization terms of the empty waveguide housing.

2.1. Multi-ridged rectangular waveguides

Following Figure 1(a), we assume that the housing contains N ridges and that their space within the cross section is defined by its lower-right coordinates (e_i , d_i) and surface areas $w_i \times t_i$.

In order to determine the TE modes of the multi-ridged waveguide, the expansion functions are identical to the modes of the housing.

$$h_{zp(m,n)} = \frac{\cos\left(\frac{m\pi}{a}x\right) \cos\left(\frac{n\pi}{b}y\right)}{\sqrt{1 + \delta_{0m}} \sqrt{1 + \delta_{0n}}} \tag{9}$$

Note that (9) satisfies all boundary conditions (δ_{0k} is the Kronecker delta) for TE modes so that matrices K_h and M_h are computed straightforwardly. Using (5), and substituting k_{xi} , k_{yi} ($m,n \rightarrow i$) and k_{xj} , k_{yj} ($l,k \rightarrow j$) for the separation constants in (9), we obtain

$$(K_h)_{ij} = [k_{xi}^2 + k_{yi}^2] \frac{ab}{4} - k_{xi}k_{xj} \sum_{n=1}^N \left\{ \int_{e_n}^{e_n+w_n} \sin(k_{xi}x) \sin(k_{xj}x) dx \int_{d_n}^{d_n+t_n} \frac{\cos(k_{yi}y)}{\sqrt{1 + \delta_{0k_{yi}}}} \frac{\cos(k_{yj}y)}{\sqrt{1 + \delta_{0k_{yj}}}} dy \right\} \\ - k_{yi}k_{yj} \sum_{n=1}^N \left\{ \int_{e_n}^{e_n+w_n} \frac{\cos(k_{xi}x)}{\sqrt{1 + \delta_{0k_{xi}}}} \frac{\cos(k_{xj}x)}{\sqrt{1 + \delta_{0k_{xj}}}} dx \int_{d_n}^{d_n+t_n} \sin(k_{yi}y) \sin(k_{yj}y) dy \right\} \tag{10a}$$

$$(M_h)_{ij} = \frac{ab}{4} \\ - \sum_{n=1}^N \left\{ \int_{e_n}^{e_n+w_n} \frac{\cos(k_{xi}x)}{\sqrt{1 + \delta_{0k_{xi}}}} \frac{\cos(k_{xj}x)}{\sqrt{1 + \delta_{0k_{xj}}}} dx \int_{d_n}^{d_n+t_n} \frac{\cos(k_{yi}y)}{\sqrt{1 + \delta_{0k_{yi}}}} \frac{\cos(k_{yj}y)}{\sqrt{1 + \delta_{0k_{yj}}}} dy \right\} \tag{10b}$$

Note that index n is used twice indicating not only the separation constant in y direction but also the number of the ridge. Therefore, we use only indices i, j in (10) and following matrix notations.

In order to determine the TM modes of the multi-ridge structure, we cannot directly use the eigenmodes of the empty waveguide housing as expansion functions since they do not satisfy the boundary conditions. Therefore, empty waveguide TM modes must be modified so that they are forced to vanish over the cross sections of the ridges. This is accomplished by a negative rectangular step function, which is defined as

$$U\left(\frac{x - x_0}{\Delta x}, \frac{y - y_0}{\Delta y}\right) = \begin{cases} 0 & \begin{cases} x_0 \leq x \leq x_0 + \Delta x \\ y_0 \leq y \leq y_0 + \Delta y \end{cases} \\ 1 & \text{elsewhere} \end{cases} \tag{11}$$

and enables us to set to zero e_{zp} in (2) over the surface of the ridges.

$$e_{zp(l,k)} = \sin\left(\frac{l\pi}{a}x\right) \sin\left(\frac{k\pi}{b}y\right) \prod_{n=1}^N U\left(\frac{x - e_n}{w_n}, \frac{y - d_n}{t_n}\right) \tag{12}$$

Note that the derivatives of (12) lead to delta functions. However, they are only required to compute matrix K in (4a) and, thus, appear under an integral where applications of the sifting theorem can be used.

After substituting k_{xj} , k_{yj} ($l,k \rightarrow j$) and k_{xi} , k_{yi} ($m,n \rightarrow i$) for the separation constants in (12) and performing the related operations, the matrices K and M for TM modes in a multi-ridged

waveguide are obtained as

$$\begin{aligned}
 (K_e)_{ij} = & [k_{xi}^2 + k_{yj}^2] \frac{ab}{4} + (K_{e\delta})_{ij} \\
 & - k_{xi}k_{xj} \sum_{n=1}^N \left\{ \int_{e_n}^{e_n+w_n} \cos(k_{xi}x) \cos(k_{xj}x) dx \int_{d_n}^{d_n+t_n} \sin(k_{yi}y) \sin(k_{yj}y) dy \right\} \\
 & - k_{yi}k_{yj} \sum_{n=1}^N \left\{ \int_{e_n}^{e_n+w_n} \sin(k_{xi}x) \sin(k_{xj}x) dx \int_{d_n}^{d_n+t_n} \cos(k_{yi}y) \cos(k_{yj}y) dy \right\} \quad (13a)
 \end{aligned}$$

$$(M_e)_{ij} = \frac{ab}{4} - \sum_{n=1}^N \left\{ \int_{e_n}^{e_n+w_n} \sin(k_{xi}x) \sin(k_{xj}x) dx \int_{d_n}^{d_n+t_n} \sin(k_{yi}y) \sin(k_{yj}y) dy \right\} \quad (13b)$$

Note that matrix $K_{e\delta}$ in (13a) is related to applying the sifting theorem in (4a). It contains combinations of the line integrals on the surface of the ridges in one direction multiplied by the terms from the sifting theorem in the respective other direction.

$$\begin{aligned}
 (K_{e\delta})_{ij} = & \sum_{n=1}^N \{ \sin(k_{xi}e_n) \sin(k_{xj}e_n) + \sin(k_{xi}(e_n + w_n)) \sin(k_{xj}(e_n + w_n)) \\
 & + k_{xj}(-\sin(k_{xi}e_n) \cos(k_{xj}e_n) + \sin(k_{xi}(e_n + w_n)) \cos(k_{xj}(e_n + w_n))) \\
 & + k_{xi}(-\cos(k_{xi}e_n) \sin(k_{xj}e_n) + \cos(k_{xi}(e_n + w_n)) \sin(k_{xj}(e_n + w_n))) \} \\
 & \times \int_{d_n}^{d_n+t_n} \sin(k_{yi}y) \sin(k_{yj}y) dy \\
 & + \sum_{n=1}^N \{ \sin(k_{yi}d_n) \sin(k_{yj}d_n) + \sin(k_{yi}(d_n + t_n)) \sin(k_{yj}(d_n + t_n)) \\
 & + k_{yj}(-\sin(k_{yi}d_n) \cos(k_{yj}d_n) + \sin(k_{yi}(d_n + t_n)) \cos(k_{yj}(d_n + t_n))) \\
 & + k_{yi}(-\cos(k_{yi}d_n) \sin(k_{yj}d_n) + \cos(k_{yi}(d_n + t_n)) \sin(k_{yj}(d_n + t_n))) \} \\
 & \times \int_{e_n}^{e_n+w_n} \sin(k_{xi}x) \sin(k_{xj}x) dx \quad (13c)
 \end{aligned}$$

This matrix, in combination with (13a), is used in (3) to calculate the TM-mode eigenvalues and the related eigenvectors.

Figure 2 shows a convergence analysis for rectangular waveguides with four ridges and comparison with fundamental-mode measurements of [1] (Figure 2(a)) and fundamental-mode calculations of [10] (Figure 2(b)). The cut-off frequencies of the multi-ridged waveguides are displayed as a function of the highest cut-off frequency in the housing up to which all terms (m, n) in (9) and (l, k) in (12) are considered. Good convergence behavior is observed for all modes in Figure 2. Obviously, the two-plane symmetric structure in Figure 2(a) requires fewer expansion terms as the symmetry also affects the number of symmetric terms in the expansions. The asymmetric cross section in Figure 2(b) requires all asymmetric expansion terms and, therefore, their numbers are much higher. Of specific interest for later three-dimensional analysis is the fact that modes with almost identical cut-off frequencies, e.g. the 2nd, 3rd and 5th, 6th TE modes in Figure 2(b), are accurately computed. Such cases have always caused problems in mode-search algorithms that require a system determinant to vanish, e.g. [3–13].

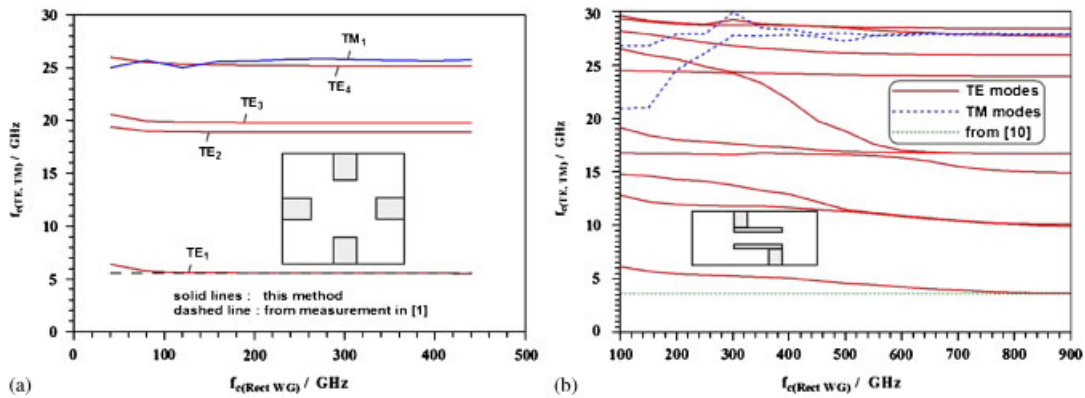


Figure 2. Convergence analysis of quadruple-ridged rectangular waveguides in symmetric (a) and asymmetric (b) configuration.

The last step towards a three-dimensional MMT analysis is the computation of the coupling matrix in (7). Whereas J_{hh} is straightforwardly obtained from (8a), a simple modification is required for J_{ee} in (8b). Here K_e differs from that in (13a) since $K_{e\delta}$ is zero. This is due to the fact that the sum of the housing's TM modes forces the transverse electric field to vanish on the face of the ridges.

Finally, coupling submatrix J_{eh} that relates the housing's TM modes (index e) to the multi-ridged waveguide's TE modes (index h), is given by

$$(J_{eh})_{q,i} = D_q \left\{ k_{xeq} \sum_{p=1}^{P_h} k_{yhp}(c_h)_{ip} \sum_{n=1}^N \int_{e_n}^{e_n+w_n} \cos(k_{xeq}x) \frac{\cos(k_{xhj}x)}{\sqrt{1 + \delta_0 k_{xhj}}} dx \int_{d_n}^{d_n+t_n} \sin(k_{yeq}y) \sin(k_{yhj}y) dy \right. \\ \left. - k_{yeq} \sum_{p=1}^{P_h} k_{xhp}(c_h)_{ip} \sum_{n=1}^N \int_{e_n}^{e_n+w_n} \sin(k_{xeq}x) \sin(k_{xhj}x) dx \int_{d_n}^{d_n+t_n} \cos(k_{yeq}y) \frac{\cos(k_{yhj}y)}{\sqrt{1 + \delta_0 k_{yhj}}} dy \right\} \quad (14)$$

From here on, standard MMT procedures are applied to obtain the overall modal scattering matrices of waveguide components involving multiple ridges.

2.2. Multi-ridged circular waveguides

For circular multi-ridged cross sections as depicted in Figure 1(b), the following expansion functions for TE and TM modes, respectively, are used

$$h_{zp(m,n)} = J_m(k_{chmn}\rho) \begin{Bmatrix} \cos(m\phi) \\ \sin(m\phi) \end{Bmatrix} \quad (15)$$

$$e_{zp(l,k)} = J_l(k_{celk}\rho) \begin{Bmatrix} \sin(l\phi) \\ \cos(l\phi) \end{Bmatrix} \prod_{n=1}^N U\left(\frac{\rho - \rho_n}{\Delta\rho_n}, \frac{\phi - \phi_n}{\Delta\phi_n}\right) \quad (16)$$

where J denotes Bessel functions of the first kind, $k_{ch,e}$ are the well-known cut-off wavenumbers in the empty housing, and function U is the circular equivalent to (11). The K and M matrices used in (3) are $(m,n \rightarrow i; l,k \rightarrow j)$.

For *TE modes*

$$(K_h)_{ij} = \frac{1}{A_i^2} - k_{chi}k_{chj} \sum_{n=1}^N \left\{ \int_{\rho_n}^{\rho_n+\Delta\rho_n} J'_m(k_{chi}\rho)J'_l(k_{chj}\rho)\rho \, d\rho \int_{\phi_n}^{\phi_n+\Delta\phi_n} \begin{Bmatrix} \cos(m\phi) \\ \sin(m\phi) \end{Bmatrix} \begin{Bmatrix} \cos(l\phi) \\ \sin(l\phi) \end{Bmatrix} d\phi \right\} - ml \sum_{n=1}^N \left\{ \int_{\rho_n}^{\rho_n+\Delta\rho_n} J_m(k_{chi}\rho)J_l(k_{chj}\rho) \frac{d\rho}{\rho} \int_{\phi_n}^{\phi_n+\Delta\phi_n} \begin{Bmatrix} \sin(m\phi) \\ \cos(m\phi) \end{Bmatrix} \begin{Bmatrix} \sin(l\phi) \\ \cos(l\phi) \end{Bmatrix} d\phi \right\} \tag{17a}$$

$$(M_h)_{ij} = \frac{1}{(A_i k_{chi})^2} - \sum_{n=1}^N \left\{ \int_{\rho_n}^{\rho_n+\Delta\rho_n} J_m(k_{chi}\rho)J_l(k_{chj}\rho)\rho \, d\rho \int_{\phi_n}^{\phi_n+\Delta\phi_n} \begin{Bmatrix} \cos(m\phi) \\ \sin(m\phi) \end{Bmatrix} \begin{Bmatrix} \cos(l\phi) \\ \sin(l\phi) \end{Bmatrix} d\phi \right\} \tag{17b}$$

where indices m, l are the respective orders of Bessel functions appearing in orders i, j of increasing wavenumbers of the circular housing, the prime denotes the derivative with respect to the argument, and A_i is the normalization coefficient

$$A_{(i \rightarrow m,n)} = \sqrt{\frac{2}{\pi(1 + \delta_{om})}} \frac{1}{\sqrt{x'^2_{mn} - m^2} J_m(x'_{mn})} \tag{17c}$$

with x'_{mn} being the n th zero of the derivative of J_m .

For *TM modes*, we obtain

$$(K_e)_{ij} = \frac{1}{D_i^2} - (K_{e\delta})_{ij} - k_{cei}k_{cej} \sum_{n=1}^N \left\{ \int_{\rho_n}^{\rho_n+\Delta\rho_n} J'_m(k_{cei}\rho)J'_l(k_{cej}\rho)\rho \, d\rho \int_{\phi_n}^{\phi_n+\Delta\phi_n} \begin{Bmatrix} \sin(m\phi) \\ \cos(m\phi) \end{Bmatrix} \begin{Bmatrix} \sin(l\phi) \\ \cos(l\phi) \end{Bmatrix} d\phi \right\} - ml \sum_{n=1}^N \left\{ \int_{\rho_n}^{\rho_n+\Delta\rho_n} J_m(k_{cei}\rho)J_l(k_{cej}\rho) \frac{d\rho}{\rho} \int_{\phi_n}^{\phi_n+\Delta\phi_n} \begin{Bmatrix} \cos(m\phi) \\ -\sin(m\phi) \end{Bmatrix} \begin{Bmatrix} \cos(l\phi) \\ -\sin(l\phi) \end{Bmatrix} d\phi \right\} \tag{18a}$$

$$(M_e)_{ij} = \frac{1}{(D_i k_{cei})^2} - \sum_{n=1}^N \left\{ \int_{\rho_n}^{\rho_n+\Delta\rho_n} J_m(k_{cei}\rho)J_l(k_{cej}\rho)\rho \, d\rho \int_{\phi_n}^{\phi_n+\Delta\phi_n} \begin{Bmatrix} \sin(m\phi) \\ \cos(m\phi) \end{Bmatrix} \begin{Bmatrix} \sin(l\phi) \\ \cos(l\phi) \end{Bmatrix} d\phi \right\} \tag{18b}$$

$$D_{(i \rightarrow m,n)} = \sqrt{\frac{2}{\pi(1 + \delta_{om})}} \frac{1}{x_{mn} J_m(x_{mn})} \tag{18c}$$

with x_{mm} being the n th zero of J_m . Matrix elements $(K_{e\delta})_{ij}$ in (18a) are given as

$$\begin{aligned}
 (K_{e\delta})_{ij} = & \sum_{n=1}^N \{ \rho_n (J_m(k_{cei}\rho_n)J_l(k_{cej}\rho_n) - k_{cej}J_m(k_{cei}\rho_n)J'_l(k_{cej}\rho_n) - k_{cei}J'_m(k_{cei}\rho_n)J_l(k_{cej}\rho_n)) \\
 & + (\rho_n + \Delta\rho_n)J_m(k_{cei}(\rho_n + \Delta\rho_n))J_l(k_{cej}(\rho_n + \Delta\rho_n)) \\
 & - (\rho_n + \Delta\rho_n)k_{cej}J_m(k_{cei}(\rho_n + \Delta\rho_n))J'_l(k_{cej}(\rho_n + \Delta\rho_n)) \\
 & - (\rho_n + \Delta\rho_n)k_{cei}J'_m(k_{cei}(\rho_n + \Delta\rho_n))J_l(k_{cej}(\rho_n + \Delta\rho_n)) \} \\
 & \times \int_{\phi_n}^{\phi_n + \Delta\phi_n} \left\{ \begin{matrix} \sin(m\phi) \\ \cos(m\phi) \end{matrix} \right\} \left\{ \begin{matrix} \sin(l\phi) \\ \cos(l\phi) \end{matrix} \right\} d\phi \\
 & + \sum_{n=1}^N \left\{ \left\{ \begin{matrix} \sin(m\phi_n) \\ \cos(m\phi_n) \end{matrix} \right\} \left\{ \begin{matrix} \sin(l\phi_n) \\ \cos(l\phi_n) \end{matrix} \right\} - l \left\{ \begin{matrix} \sin(m\phi_n) \\ \cos(m\phi_n) \end{matrix} \right\} \left\{ \begin{matrix} \cos(l\phi_n) \\ -\sin(l\phi_n) \end{matrix} \right\} \right. \\
 & - m \left\{ \begin{matrix} \cos(m\phi_n) \\ -\sin(m\phi_n) \end{matrix} \right\} \left\{ \begin{matrix} \sin(l\phi_n) \\ \cos(l\phi_n) \end{matrix} \right\} + \left. \left\{ \begin{matrix} \sin(m(\phi_n + \Delta\phi_n)) \\ \cos(m(\phi_n + \Delta\phi_n)) \end{matrix} \right\} \left\{ \begin{matrix} \sin(l(\phi_n + \Delta\phi_n)) \\ \cos(l(\phi_n + \Delta\phi_n)) \end{matrix} \right\} \right. \\
 & + l \left\{ \begin{matrix} \sin(m(\phi_n + \Delta\phi_n)) \\ \cos(m(\phi_n + \Delta\phi_n)) \end{matrix} \right\} \left\{ \begin{matrix} \cos(l(\phi_n + \Delta\phi_n)) \\ -\sin(l(\phi_n + \Delta\phi_n)) \end{matrix} \right\} \\
 & \left. + m \left\{ \begin{matrix} \cos(m(\phi_n + \Delta\phi_n)) \\ -\sin(m(\phi_n + \Delta\phi_n)) \end{matrix} \right\} \left\{ \begin{matrix} \sin(l(\phi_n + \Delta\phi_n)) \\ \cos(l(\phi_n + \Delta\phi_n)) \end{matrix} \right\} \right\} \int_{\rho_n}^{\rho_n + \Delta\rho_n} J_m(k_{cei}\rho)J_l(k_{cej}\rho) \frac{d\rho}{\rho}
 \end{aligned}
 \tag{18d}$$

Note that what was stated for rectangular multi-ridges regarding matrices J_{ee} , K_e and $K_{e\delta}$, applies in the same way to the circular multi-ridge case. Finally, the coupling submatrix J_{eh} is computed from

$$\begin{aligned}
 (J_{eh})_{q,i} = & D_q \left\{ k_{ceq} \sum_{p=1}^{P_h} l(c_h)_{ip} \sum_{n=1}^N \int_{\rho_n}^{\rho_n + \Delta\rho_n} J'_m(k_{ceq}\rho)J_l(k_{chj}\rho) d\rho \right. \\
 & \times \int_{\phi_n}^{\phi_n + \Delta\phi_n} \left\{ \begin{matrix} \sin(m\phi) \\ \cos(m\phi) \end{matrix} \right\} \left\{ \begin{matrix} -\sin(l\phi) \\ \cos(l\phi) \end{matrix} \right\} d\phi - m \sum_{p=1}^{P_h} k_{chj}(c_h)_{ip} \\
 & \left. \times \sum_{n=1}^N \int_{\rho_n}^{\rho_n + \Delta\rho_n} J_m(k_{ceq}\rho)J'_l(k_{chj}\rho) d\rho \int_{\phi_n}^{\phi_n + \Delta\phi_n} \left\{ \begin{matrix} \cos(m\phi) \\ -\sin(m\phi) \end{matrix} \right\} \left\{ \begin{matrix} \cos(l\phi) \\ \sin(l\phi) \end{matrix} \right\} d\phi \right\}
 \end{aligned}
 \tag{19}$$

Of course, the individual sine and cosine functions in (17)–(19) are valid only for their respective cross-sectional symmetries. For asymmetric circular multi-ridged cross sections such as depicted in Figure 1(b), all four possible combinations must be considered.

This completes the presentation of the theory. Among the many advantages outlined in the introduction section, one serious disadvantage of this method must be addressed. With increasing cross-sectional area occupied by the ridges within the housing’s cross section and with an increasing number of expansion terms in (2), the symmetric matrices in (4a) and (4b) become ill-conditioned. As a result, matrix M is no longer positive definite, which can be immediately detected by an appropriate eigenvalue/vector-solving code. In such cases, an adaptive process must be used to find a reasonable compromise between accuracy and computational efficiency.

As an example, consider a rectangular waveguide with aspect ratio $a = 2b$ containing a single ridge of height $b/2$ and variable width. As the ridge width increases from $a/10$ to $2a/3$, the maximum solvable eigenvalue matrix size decreases from above 2000 to 185. Good convergence is reached at a size of about 300, which can be maintained up to a width of $a/3$. At a width of $2a/3$ and matrix size of 185, the fundamental-mode cut-off frequency is only a single percent higher than that calculated with a MMT-based singular-value solver.

For all practical applications and certainly for those presented in the next section, eigenmode solutions converge sufficiently well before this effect comes into play.

3. RESULTS

Before comparing the eigenvalue mode-spectrum analysis of multiple-ridged cross-section waveguides with other numerical techniques, agreement with measurements is demonstrated. Figure 3 presents the input reflection coefficient in dB of a back-to-back rectangular-to-ridge waveguide transformer. The results of our technique (solid line) are in very good agreement with the MMT (dashed line) and measurements (crosses) presented in [4]. Note that the analysis of this component requires the computation of six different double-ridge waveguide mode spectra. Differences between the three results in Figure 4 are small and well below -25 dB; therefore, they are acceptable in almost all practical applications.

Figure 4 shows the performance of the below-cutoff T-septum waveguide filter at 2.15 GHz as proposed in [6]. Excellent agreement is obtained with the results of an approach that combines the Coupled Integration-Equation Technique (CIET) with the MMT. Especially the passband peaks at 7.6 and 7.8 GHz are accurately reproduced, which attests to an accurate calculation of the mode spectrum of the T-septum waveguide sections. Excellent agreement of the $|S_{11}|$ and group-delay performances between 2 GHz and 2.3 GHz has already been documented in [30]. We refrain from repeating these results and refer the reader to [30].

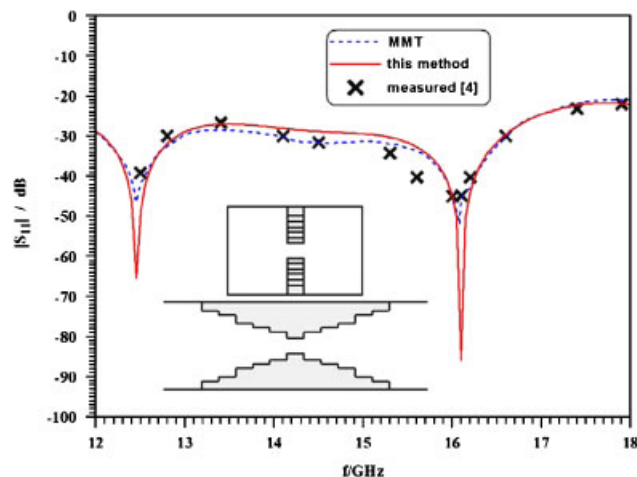


Figure 3. Back-to-back rectangular-to-ridge waveguide transformer: Comparison of the results of this method (solid line) with those obtained by the MMT (dashed line) and measurements [4].

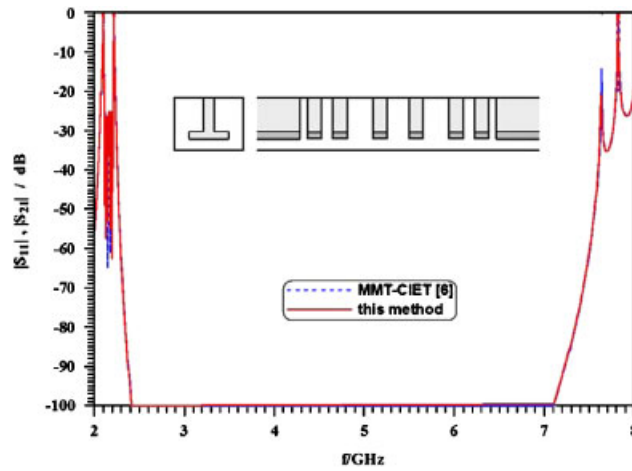


Figure 4. Performance of a below-cutoff T-septum waveguide filter: This method (solid lines), CIET–MMT (dashed lines) [6].

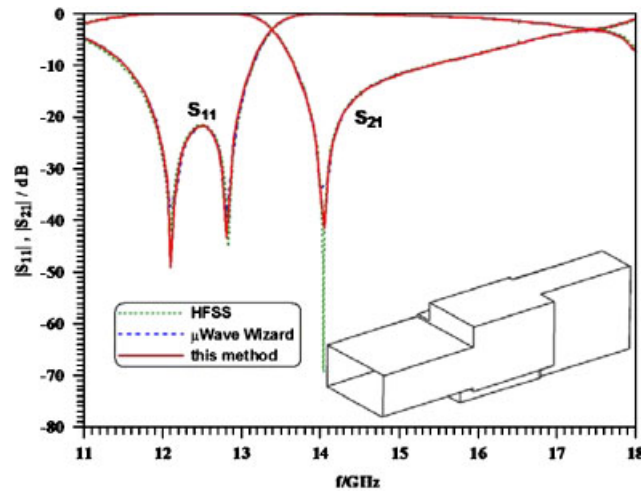


Figure 5. Performance of a 90° rectangular waveguide twist: This method (solid lines), μWave Wizard (dashed lines), Ansoft HFSS (dotted lines).

As the MMT analysis in axial direction is identical in both methods, only the time for the computation of the T-septum waveguide mode spectrum and the coupling matrix needs to be compared. For this structure, the method proposed here runs approximately 2.5 times longer than the CIET–MMT. This appears to be a disadvantage. However, with comparable effort, our method produces reliable results for a cross section, in which ridges occupy opposite corners of a rectangular housing (c.f. inset of Figure 5). A three-dimensional analysis of this twist based solely on the MMT has not been presented so far as it causes serious numerical complications in

the power normalization of the individual modes. This is one of the reasons why both commercial software packages used to verify our results in Figure 5 employ the finite-element method for the mode-spectrum analysis.

The 90° waveguide twist component shown in Figure 5 is designed for operation between 12 and 13 GHz. It must be analyzed/optimized by a full set of modes as its center cross section is asymmetric. The excellent agreement of our results (solid lines) with those of the μ Wave Wizard[®] (dashed lines) and Ansoft HFSS[®] (dotted lines) demonstrates that our eigenvalue technique correctly computes waveguide components involving different polarizations. Note that the twist can also be viewed as a filter, where the two lowest modes in the ridged guide provide the two resonances at 12.1 and 12.8 GHz. The attenuation pole at 14 GHz is produced by bypass coupling from the input to the second resonance, which is identical to that from the first resonance to the output.

We now turn our attention to circular ridged waveguide components. Figure 6 shows the performance of a double-ridge waveguide between two standard circular waveguides. The reflection coefficients for vertical and horizontal polarizations are plotted along with the phase difference between the two polarizations. This can be achieved by either separately using the two (cosine and sine) polarizations given in (15)–(19) or by using only one of the two and performing two separate calculations, with the positions of the ridges rotated by 90° in the second run. The excellent agreement of our results (solid lines) in magnitude and phase with those obtained with the MMT (e.g. [13]) validates the eigenvalue analysis for multi-ridged circular waveguides.

A direct application of the structure in Figure 6 is a circular ridged waveguide polarizer [13] as shown in Figure 7. The component is designed for operation between 19 and 22 GHz with the following specifications: 30 dB return loss and isolation, 0.75 dB axial ratio. Excellent agreement of those parameters with results from the MMT is demonstrated and validates the eigenvalue technique presented here.

The last example, shown in Figure 8, is a four-pole below-cutoff circular ridge waveguide filter, where the empty circular waveguide sections are used as coupling elements between the

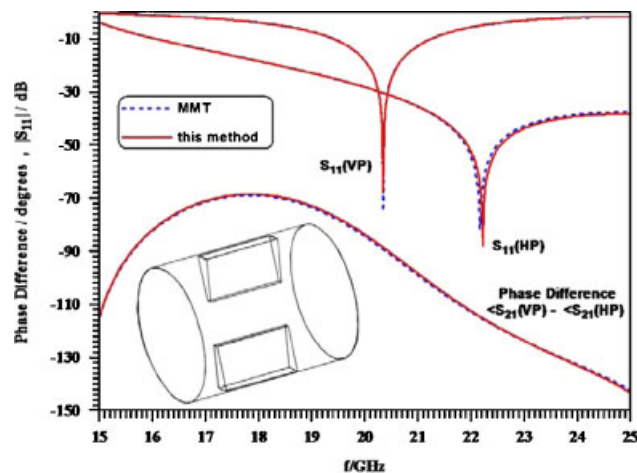


Figure 6. Double-ridge section in circular waveguide: This method (solid lines), MMT (dashed lines).

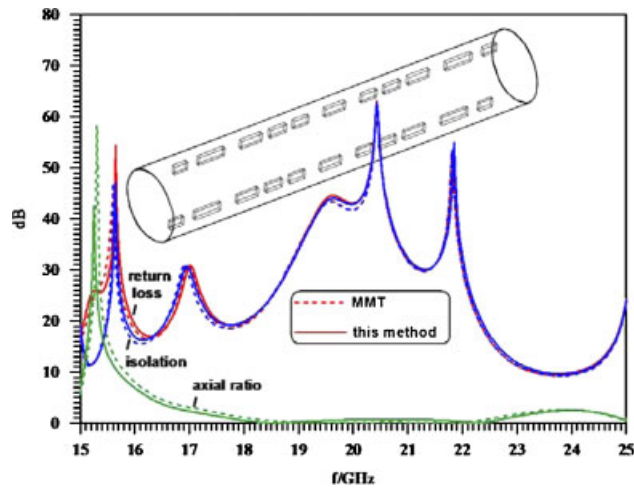


Figure 7. Performance of a circular ridged waveguide polarizer with 11 double-ridge sections: This method (solid lines), MMT (dashed lines).

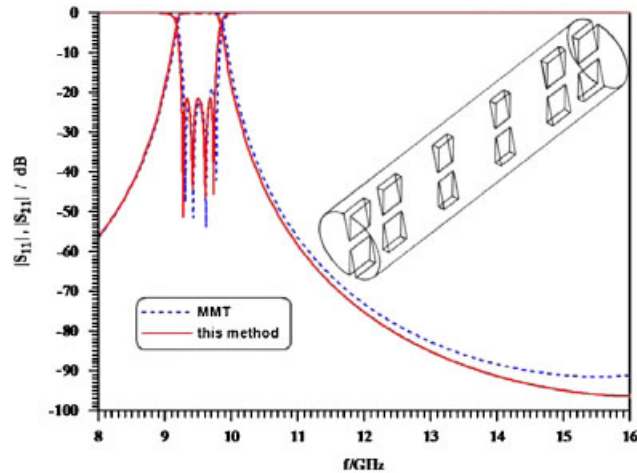


Figure 8. Performance of a four-pole below-cutoff circular ridge waveguide filter: This method (solid lines), MMT (dashed lines).

ridge waveguide resonators and input/output ports. The Chebyshev-type design features a 500 MHz, 22 dB return-loss bandwidth centered at 9.5 GHz and shows good stopband behavior up to 16 GHz and beyond. The performance of this filter is validated by results obtained from an MMT code as used in [13]. Only very slight discrepancies between the two sets of curves are observed and are attributed to the fact that the number of expansion terms used in the MMT code had to be limited for numerical stability. Thus, this example shows that the eigenvalue technique is well suited for ridge waveguide circuit design.

4. CONCLUSIONS

The classical eigenvalue mode-spectrum analysis presents a viable alternative for the design of narrowband waveguide components formed by waveguides involving multi-ridged cross sections. The theory is presented for multiple ridges in rectangular and circular enclosures. Its validity is verified by comparisons with mode-matching-based codes, commercially available full-wave field solvers and measurements. Although this technique is computationally slower than comparable MMT algorithms, its advantage lies in the flexible selection of all locations and the number of ridges in a waveguide housing. Therefore, it makes possible the three-dimensional analysis and design of related components by a strictly modal-based approach and refrains from introducing hybrid numerical techniques.

REFERENCES

1. Sun W, Balanis CA. Analysis and design of quadruple-ridged waveguides. *IEEE Transactions on Microwave Theory and Techniques* 1994; **42**:2201–2207.
2. Tang Y, Zhao J, Wu W. Analysis of quadruple-ridged square waveguide by multilayer perceptron neural network model. *Proceedings of the Asia-Pacific Microwave Conference*, Yokohama, Japan, December 2006; 1912–1918.
3. Bornemann J, Arndt F. Transverse resonance, standing wave, and resonator formulations of the ridge waveguide eigenvalue problem and its application to the design of E-plane finned waveguide filters. *IEEE Transactions on Microwave Theory and Techniques* 1990; **38**:1104–1113.
4. Bornemann J, Arndt F. Modal-S-matrix design of optimum stepped ridged and finned waveguide transformers. *IEEE Transactions on Microwave Theory and Techniques* 1987; **35**:561–567.
5. Rong Y, Zaki KA. Characteristics of generalized rectangular and circular ridge waveguides. *IEEE Transactions on Microwave Theory and Techniques* 2000; **48**:258–265.
6. Labay VA, Bornemann J, Amari S, Damaschke JM. Direct-coupled waveguide filters for the lower gigahertz frequency range. *International Journal of RF and Microwave Computer-aided Engineering* 2002; **12**:217–225.
7. Zhan Y, Joines W. Some properties of T-septum waveguides. *IEEE Transactions on Microwave Theory and Techniques* 1987; **35**:769–775.
8. Pauplis BE, Power DC. On the bandwidth of T-septum waveguide. *IEEE Transactions on Microwave Theory and Techniques* 1989; **31**:919–922.
9. Labay VA, Bornemann J. Singular value decomposition improves accuracy and reliability of T-septum waveguide field-matching analysis. *International Journal of Microwave Millimeter-wave Computer-aided Engineering* 1992; **2**:82–89.
10. Saha PK, Guha D. New broadband rectangular waveguide with L-shaped septa. *IEEE Transactions on Microwave Theory and Techniques* 1992; **40**:777–781.
11. Guha D, Saha PK. Some characteristics of ridge-trough waveguide. *IEEE Transactions on Microwave Theory and Techniques* 1997; **45**:449–453.
12. Balaji U, Vahldieck R. Radial mode matching analysis of ridged circular waveguides. *IEEE Transactions on Microwave Theory and Techniques* 1996; **44**:1183–1186.
13. Bornemann J, Amari S, Uher J, Vahldieck R. Analysis and design of circular ridged waveguide components. *IEEE Transactions on Microwave Theory and Techniques* 1999; **47**:330–335.
14. Morini A, Rozzi T, Angeloni A. Accurate calculation of the modes of the circular multiridge waveguide. *IEEE MTT-S International Microwave Symposium Digest*, Denver, U.S.A., June 1997; 199–202.
15. Zhang HZ, James GL. Characteristics of quad-ridged coaxial waveguides for dual-band horn applications. *IEE Proceedings—Microwave Antennas and Propagation* 1998; **145**:225–228.
16. Zhang HZ. A wideband orthogonal-mode junction using a junction of a quad-ridged coaxial waveguide and four sectoral waveguides. *IEEE Microwave and Wireless Components Letters* 2002; **12**:172–174.
17. Serebryannikov AE, Vasylychenko OE, Schuenemann K. Fast coupled-integral-equations-based analysis of azimuthally corrugated cavities. *IEEE Microwave and Wireless Components Letters* 2004; **14**:240–242.
18. Komarov VV. Classification of metallic waveguides with complex cross-sections. *IEE Proceedings—Microwave Antennas and Propagation* 2001; **148**:398–402.
19. Swaminathan M, Arvas E, Sakar TK, Djordjevic AR. Computation of cutoff wave numbers of TE and TM modes in waveguides of arbitrary cross sections using a surface integral formulation. *IEEE Transactions on Microwave Theory and Techniques* 1990; **38**:154–159.

20. Cogollos S, Marini S, Boria VE, Soto P, Vidal A, Esteban H, Morro JV, Gimeno B. Efficient modal analysis of arbitrarily shaped waveguides composed of linear, circular, and elliptical arcs using the BI-RME method. *IEEE Transactions on Microwave Theory and Techniques* 2003; **51**:2378–2390.
21. Lucido M, Panariello G, Schettino F. Full wave analysis of arbitrary polygonal section waveguides. *IEEE MTT-S International Microwave Symposium Digest*, Honolulu, U.S.A., 2007; 2033–2036.
22. Conciauro G, Bressan M, Zuffada C. Waveguide modes via an integral equation leading to a linear matrix eigenvalue problem. *IEEE Transactions on Microwave Theory and Techniques* 1984; **32**:1495–1504.
23. Omar AS, Schünemann KF. Analysis of waveguides with metal inserts. *IEEE Transactions on Microwave Theory and Techniques* 1989; **37**:1924–1932.
24. Omar AS, Schünemann KF. Applications of the generalized spectral-domain technique to the analysis of rectangular waveguides with rectangular and circular metal inserts. *IEEE Transactions on Microwave Theory and Techniques* 1991; **39**:944–952.
25. Beyer R, Arndt F. Efficient modal analysis of waveguide filters including the orthogonal mode coupling elements by an MM/FE method. *IEEE Microwave and Guided Wave Letters* 1995; **5**:9–11.
26. Lin S-L, Li L-W, Yeo T-S, Leong M-S. Cutoff wavenumbers in truncated waveguides. *IEEE Microwave and Wireless Components Letters* 2001; **11**:214–216.
27. Lin S-L, Li L-W, Yeo T-S, Leong M-S. Analysis of metallic waveguides of a large class of cross sections using polynomial approximation and superquadratic functions. *IEEE Transactions on Microwave Theory and Techniques* 2001; **49**:1136–1139.
28. Lin SL, Li LW, Yeo TS, Leong MS. Novel modified mode matching analysis of concentric waveguide junctions. *IEE Proceedings—Microwave Antennas and Propagation* 2001; **148**:369–374.
29. Li L-W, Lin S-W, Yeo T-S, Leong M-S. Modal analysis of waveguides and efficient CAD of waveguide junctions using a unified method. *Proceedings of the Asia-Pacific Microwave Conference*, Taipei, Taiwan, December 2001; 433–436.
30. Yu SY, Bornemann J. Mode spectrum eigenvalue formulation for irregular waveguides and its application to waveguide component design. *Proceedings of the German Microwave Conference (GeMiC)*, Hamburg, Germany, March 2008; 360–363.

AUTHORS' BIOGRAPHIES



Seng Yong Yu received the BSc degree from the Department of Physics, East China Normal University, Shanghai, China in 1985, the MSc degree from the Department of Physics, Kumamoto University, Kyushu, Japan in 1996 and the PhD degree from the Department of Electrical and Computer Engineering, University of Victoria, Victoria, BC, Canada, in 2008.

From 1985 to 1994, he worked as an electronic engineer in the Shanghai Shipbuilding Industry Co. From 1994 to 1997, he was a assistant research engineer in the Physics Laboratory of Kumamoto University, where he was mainly engaged in the design and development of cryogenic laser devices for spectroscopy. Since January 2009, he is a Postdoctoral Fellow at the University of Victoria. His research interests include numerical analysis and techniques in electromagnetics, modeling of guided-wave structures, computer-aided design, and efficient optimization using frequency domain simulation methods for various applications.



Jens Bornemann received the Dipl.-Ing. and the Dr.-Ing. degrees, both in electrical engineering, from the University of Bremen, Germany, in 1980 and 1984, respectively.

From 1984 to 1985, he was a consulting engineer. In 1985, he joined the University of Bremen, Germany, as an Assistant Professor. Since April 1988, he has been with the Department of Electrical and Computer Engineering, University of Victoria, Victoria, B.C., Canada, where he became a Professor in 1992. From 1992 to 1995, he was a Fellow of the British Columbia Advanced Systems Institute. In 1996, he was a Visiting Scientist at Spar Aerospace Limited (now MDA Space), Ste-Anne-de-Bellevue, Quebec, Canada, and a Visiting Professor at the Microwave Department, University of Ulm, Germany. From 1997 to 2002, he was a co-director of the Center for Advanced Materials and Related Technology (CAMTEC), University of

Victoria. From 1999 to 2002, he served as an Associate Editor of the *IEEE Transactions on Microwave Theory and Techniques* in the area of Microwave Modeling and CAD. In 2003, he was a Visiting Professor at the Laboratory for Electromagnetic Fields and Microwave Electronics, ETH Zurich, Switzerland. From 1999 to 2008, he served on the Technical Program Committee of the *IEEE MTT-S International Microwave Symposium*. He has coauthored *Waveguide Components for Antenna Feed Systems. Theory and Design* (Artech House, 1993) and has authored/coauthored more than 220 technical papers. His research activities include RF/wireless/microwave/millimeter-wave components and systems design, and field-theory-based modeling of integrated circuits, feed networks and antennas.

Dr Bornemann is a Registered Professional Engineer in the Province of British Columbia, Canada. He is a Fellow IEEE and serves on the Editorial Board of the *International Journal of Numerical Modelling*.